FEMS Microbiology Ecology, 92, 2016, fiw088

doi: 10.1093/femsec/fiw088
Advance Access Publication Date: 27 April 2016
Research Article

RESEARCH ARTICLE

Variation in coastal Antarctic microbial community composition at sub-mesoscale: spatial distance or environmental filtering?

Mario Moreno-Pino[1], Rodrigo De la Iglesia[2,3], Nelson Valdivia[4,5], Carlos Henríquez-Castilo[2,3,6], Alexander Galán[7], Beatriz Díez[2,8] and Nicole Trefault[1,*]

[1]Center for Genomics and Bioinformatics, Faculty of Sciences, Universidad Mayor, Camino La Pirámide 5750, Santiago 8580745 Chile, [2]Department of Molecular Genetics and Microbiology, Pontificia Universidad Católica de Chile, Alameda 340, Santiago 8331150, Chile, [3]Millennium Institute of Ocenography. Cabina 7, Barrio Universitario s/n, Concepción 4030000, Chile, [4]Instituto de Ciencias Marinas y Limnológicas, Facultad de Ciencias, Universidad Austral de Chile, Campus Isla Teja, Valdivia 5090000, Chile,, [5]Centro de Investigación FONDAP: Dinámica de Ecosistemas Marinos de Altas Latitudes (IDEAL), Campus Isla Teja, Valdivia 5090000, Chile, [6]Department of Oceanography, Universidad de Concepción, Cabina 7, Barrio Universitario s/n, Concepción 4030000, Chile, [7]CREA – Centro Regional de Estudios Ambientales, Universidad Católica de la Santísima Concepción, Av. Colón 2766, Talcahuano 4270789, Chile and [8]Center for Climate and Resilience Research (CR)[2], Blanco Encalada 22002, Santiago 8370449, Chile

*Corresponding author: Center for Genomics and Bioinformatics, Faculty of Sciences, Universidad Mayor, Camino La Pirámide 5750, Huechuraba, Santiago 8580745, Chile. Tel: +56-2-25189205; E-mail: nicole.trefault@umayor.cl

One sentence summary: Coastal Antarctic photosynthetic eukaryote and bacterial communities respond differentially to environmental filtering at submesoscale.

Editor: Josef Elster

ABSTRACT

Spatial environmental heterogeneity influences diversity of organisms at different scales. Environmental filtering suggests that local environmental conditions provide habitat-specific scenarios for niche requirements, ultimately determining the composition of local communities. In this work, we analyze the spatial variation of microbial communities across environmental gradients of sea surface temperature, salinity and photosynthetically active radiation and spatial distance in Fildes Bay, King George Island, Antarctica. We hypothesize that environmental filters are the main control of the spatial variation of these communities. Thus, strong relationships between community composition and environmental variation and weak relationships between community composition and spatial distance are expected. Combining physical characterization of the water column, cell counts by flow cytometry, small ribosomal subunit genes fingerprinting and next generation sequencing, we contrast the abundance and composition of photosynthetic eukaryotes and heterotrophic bacterial local communities at a submesoscale. Our results indicate that the strength of the environmental controls differed markedly between eukaryotes and bacterial communities. Whereas eukaryotic photosynthetic assemblages responded

Received: 1 November 2015; **Accepted:** 22 April 2016

weakly to environmental variability, bacteria respond promptly to fine-scale environmental changes in this polar marine system.

Keywords: spatial variation; Antarctica; microbial community; environmental filtering; submesoscale; community composition

INTRODUCTION

Understanding the extent to which spatial environmental heterogeneity influences diversity of organisms at different scales is a key question in community ecology (Hanson *et al.* 2012; Sutherland *et al.* 2013). One of the mechanisms proposed to explain such influence is environmental filtering, by which different species can co-occur based on shared tolerances or requirements on a particular environment. Polar systems are particularly interesting to test this type of processes, since global change effects, such as rise in temperatures, melting ice and increased sea level, are occurring faster than in other sites of the planet (Clarke *et al.* 2007). In Antarctica, due to its responses to global change and a high environmental heterogeneity caused by climate disturbances, strong environmental gradients at small spatial scales—like in coastal lagoons and small bays—can be observed. This fine-scale environmental variability has been suggested to influence Antarctic biodiversity of macrobial (e.g. Valdivia *et al.* 2014) and microbial communities (e.g. Webster and Negri 2006; Verleyen *et al.* 2010).

Marine microorganisms play central roles in all marine biogeochemical process (Karl and Proctor 2007; Falkowski, Fenchel and Delong 2008). They influence climate mainly through the cycling of climate-active gases (carbon dioxide, methane, nitrous oxide and dimethyl sulfide) (Singh *et al.* 2010; Mohapatra *et al.* 2013), are responsible of nearly half of the carbon fixed on the planet (Behrenfeld *et al.* 2001), and structure healthy and stressed marine ecosystems (Azam and Worden 2004). Hence, determining the role of environmental filtering in structuring microbial Antarctic communities will improve our predictions of the functional response of marine ecosystems to environmental changes.

The metacommunity framework explicitly incorporates the effect of environmental filtering—in addition to dispersal and species interactions—on the structure and composition of local communities (Holyoak, Leibold and Holt 2005; Logue *et al.* 2011). This environmental filtering or species sorting perspective is similar to the Baas-Becking hypothesis (Baas-Becking 1934) for microbial communities and suggests that local environmental conditions provide habitat-specific scenarios for niche requirements, ultimately determining the composition of local communities. Therefore, dispersal among habitats should be high enough to allow species to fill niches in habitat patches (Holyoak, Leibold and Holt 2005). Considering that the major dispersal vehicle of microorganisms in the ocean is water-mass movement, it can be suggested that dispersal potential of microbial communities might be quite high. Recent observations in subpolar and Arctic waters indicate that environmental filtering explains some, but not all, components of the microbial community (Winter, Matthews and Suttle 2013). Accordingly, the whole microbial community (i.e. Bacteria, Archaea and Eukarya) and their interactions with the environment should be analyzed simultaneously toward a comprehensive understanding of community regulation.

While the vast majority of polar marine studies on spatial variation of microbial communities have focused on the bacterial (e.g. Ghiglione *et al.* 2012; Winter, Matthews and Suttle 2013) or the eukaryote component (Díez *et al.* 2004; Jiang *et al.* 2014; Lee *et al.* 2014) just few have analyzed both microbial components in the same analysis (Luria, Ducklow and Amaral-Zettler 2014). Antarctic marine waters are dominated by two key microbial functional groups: a well-known bacterial component, in which photosynthetic bacteria are considered absent, and a less studied photosynthetic eukaryote group, responsible for fueling marine trophic networks (reviewed in De la Iglesia and Trefault 2012 and Wilkins *et al.* 2013). Antarctic bacterioplankton assemblages are dominated by Alphaproteobacteria, specifically by the worldwide-distributed SAR11 clade, and by Gammaproteobacteria, represented by SAR86 clade, member of the Oceanospirillales order (López-García *et al.* 2001; Piquet *et al.* 2011; Grzymski *et al.* 2012). In the photosynthetic eukaryote group, a prevailing trend observed is that diatoms such as *Thalassiosira* spp. and *Chaetoceros* spp. generally dominate during the development of stratified conditions, while flagellates such as *Cryptomonas* sp. and *Phaeocystis antarctica*, dominate in deeply mixed waters (Arrigo *et al.* 1999).

While bacteria are capable of tolerating a wide range of environmental forcing, such as temperature, pH, DOM, POM, salinity and nutrients (Azam and Malfatti 2007), photosynthetic eukaryotes are strongly affected by light and temperature (Ardyna *et al.* 2011; Monier *et al.* 2014). In Antarctic shores and bays, glacier melting and animal settlements significantly affect salinity (water density), light penetration and nutrient inputs into the water column (Dierssen, Smith and Vernet 2002; Sailley *et al.* 2013), which can differentially affect the bacterial and photosynthetic eukaryote components of the microbial marine community (Piquet *et al.* 2011). Fildes Bay (also known as Maxwell Bay) is located between the southwest part and northeast margins of the Nelson and King George Islands, respectively (Fig. 1). The hydrographic conditions of the bay are mainly modulated by freshwater inputs from thawed drifting icebergs and from the bordering ice caps in Fildes Peninsula and Nelson Island (Chang *et al.* 1990; Yoon *et al.* 1998). Besides, this area is particularly interesting because it harbors several scientific stations with high associated anthropogenic impacts on the marine environment (Martins *et al.* 2004; Santos *et al.* 2005). In addition, the Collins Glacier and animal settlements in Nelson Island generate strong impacts in the surrounding area. All these characteristics can generate a mosaic of environmental patches, making Fildes Bay an excellent scenario for testing local-scale spatial phenomena and environmental filtering effect over microbial communities.

Here, we analyze the surface spatial variation of the community composition of photosynthetic eukaryotes and

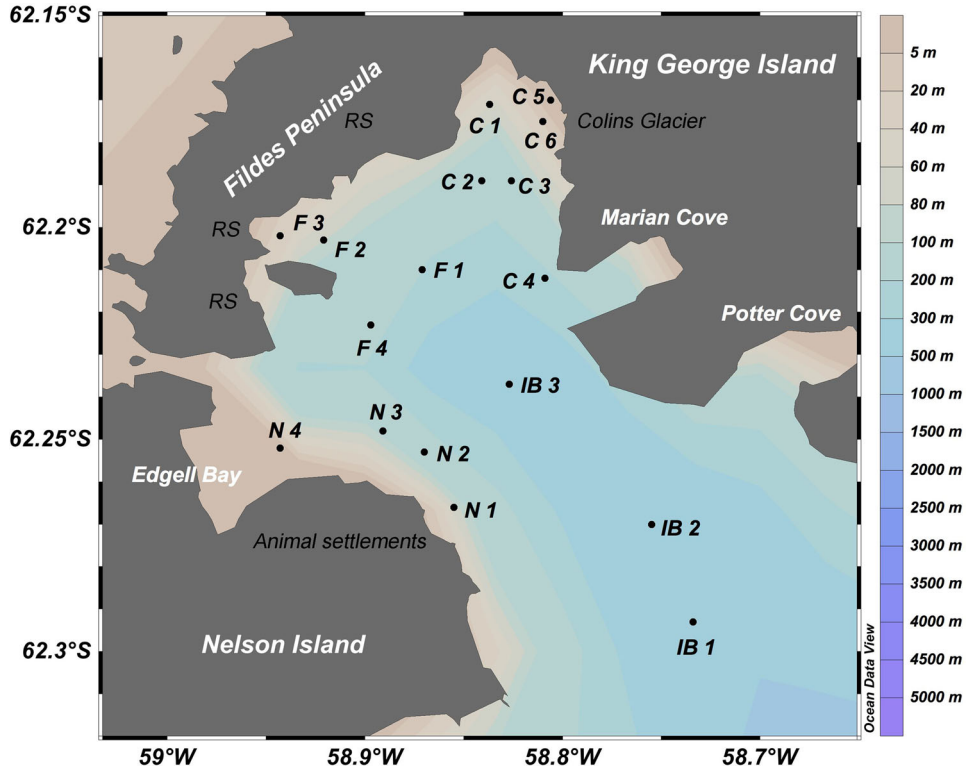

Figure 1. Geographical location of sampling area at Fildes Bay, King George Island, West Antarctic Peninsula. RS: research station.

heterotrophic bacterial microbial communities in a small Antarctic Bay. If the environmental filters are the main control of the spatial variation of these communities, strong relationships between community composition and environmental variation, but weak relationships between community composition and spatial distance are expected. In order to test this prediction, we analyzed the variation in abundance and composition of photosynthetic eukaryote and bacterial microbial communities across environmental gradients (sea surface temperature (SST), salinity and photosynthetic active radiation (PAR)) and spatial distance in Fildes Bay, King George Island, Antarctica.

MATERIAL AND METHODS

Study site and sampling

Surface water samples (5 m depth) were collected with 5 L Niskin bottles from 17 different locations at Fildes Bay, King George Island, Antarctica (Fig. 1 and Table 1), on 7 and 8 February 2012. Each location was assigned to one of the following four categories: Collins Glacier ('C' stations), Nelson Glacier ('N' stations), Fildes Bay ('F' stations) and Inner Bay ('IB' stations). Salinity, temperature, density (expressed as sigma-t) and PAR data were obtained using a CTDO SBE 911 plus (SeaBird) equipped with an auxiliary biospherycal PAR sensor (LiCor). Seawater samples (5 L) were prefiltered on board through 100 μm pore mesh and stored in acid-washed carboys and kept on dark until subsampling at the laboratory.

For community composition analysis, 5 L water samples were filtered through 0.2 μm pore size 47 mm diameter filters (GSWP04700, Millipore), using a Swinnex holder system in a Masterflex 6–600 rpm peristaltic pump (Cole Parmer). Filters were stored in 2 mL cryovials at −20°C until processed.

Photosynthetic eukaryotes and bacterial cell counts

Subsamples of 1.35 mL were taken in triplicates, fixed with 150 μL of fixative solution (10% formaldehyde, 0.5% glutaraldehyde and 100 mM sodium borate pH 8.5), incubated for 20 min at room temperature and transferred to a nitrogen dry shipper (CXR500, Taylor Wharton) until transport to the institution laboratory. For photosynthetic eukaryotes and bacterial abundance determination, events were enumerated with a 'jet-in-air' Influx flow cytometer (BD) using 488 nm blue and 640 nm red lasers combination. For photosynthetic eukaryotes enumeration, particles (hereafter called photosynthetic picoeukaryotes (PPE) and photosynthetic nanoeukaryotes (PNE1 and PNE2) were differentiated by perpendicular forward angle light scatter (FSCperp) and trigger pulse width from the 488 nm laser, and red fluorescence (692/40 nm) detection from the 488 and 640 nm lasers. For bacterial counts, subsamples (500 μL) were fixed with Sybr Green I (Invitrogen, Canada), kept in dark for 30 min and analyzed by side scattering and green fluorescence (530/20 nm), with event recording triggered on the FSCperp signal for both groups. Three micrometers fluorescent Ultra Rainbow beads (Spherotech Inc.) were used for calibration. Each sample was run at an average flow rate of 47 μL min^{-1} for 5 min for the eukaryotes and 49 μL min^{-1} for 3 min for bacteria. Analyses were performed with the FlowJo software (Tree Star).

Nucleic acids extractions and 16S rRNA gene amplification by PCR

All filter-handling steps were performed under sterile conditions. Filters were thawed in ice and half of the filters were cut into small pieces, while the other half was kept at −20°C as backup. Each sample was incubated in lysis buffer (100 mM Tris, 10 mM EDTA, pH 8.0; 0.15M NaCl), with 10% SDS and 20 mg mL^{-1}

Table 1. Geographical locations of sampling points, physicochemical parameters and microbial abundances.

Station[a]	Lat (S)	Long (W)	SST (°C)	Salinity (psu)	PAR (μmol Photons m^{-2} s^{-1})	Bacteria (10^3 Cells mL^{-1})	PPE[b]	PNE1[c] (10^2 Cells mL^{-1})	PNE2[d]
C1	62.1713	58.8367	1.90	33.9	565.9	306.42	14.46	109.81	0.85
C2	62.1885	58.8407	2.10	33.9	699.5	253.04	15.91	112.07	1.96
C3	62.1885	58.8264	1.93	34.0	599.8	185.63	14.93	112.71	1.62
C4	62.2124	58.8092	1.98	33.9	509.0	336.23	12.79	97.01	1.11
C5	62.1700	58.8059	NA[e]	NA	NA	160.35	3.20	2.47	0.04
C6	62.1750	58.8097	NA	NA	NA	236.91	17.36	53.48	2.35
F1	62.2097	58.8706	1.91	34.0	618.4	65.38	15.22	112.79	2.52
F2	62.2031	58.9209	1.64	34.1	506.1	126.17	13.09	71.22	1.45
F3	62.2017	58.9425	1.58	34.1	473.5	99.64	13.69	58.76	2.09
F4	62.2233	58.8969	1.93	34.0	129.5	384.09	8.91	75.18	2.35
IB1	62.2927	58.7341	2.02	34.0	503.1	162.51	9.04	95.86	4.56
IB2	62.2702	58.7548	2.07	34.0	184.3	279.16	9.30	91.30	4.90
IB3	62.2371	58.8271	1.88	33.8	242.3	286.63	10.62	56.97	1.92
N1	62.2661	58.8545	1.45	34.3	159.1	379.11	10.23	69.04	3.16
N2	62.2529	58.8696	1.76	34.0	212.2	553.64	14.63	52.41	1.07
N3	62.2476	58.8913	2.18	33.9	192.2	505.83	10.15	77.19	4.43
N4	62.2519	58.9426	2.29	33.9	186.0	403.12	9.30	58.00	1.07

[a]C, Collins Glacier; F, Fildes Bay (inshore); IB, Inner Bay (offshore), N: Nelson Island; [b]PPE, photosynthetic picoeukaryotes; [c]PNE1, photosynthetic nanoeukaryotes group 1; [d]PNE2, photosynthetic nanoeukaryotes group 2; [e]non available.

proteinase K and incubated at 37°C for 1 h. DNA was extracted using 5 M NaCl and N-cetyl N,N,N-trimethylammonium bromide (CTAB) extraction buffer (10% CTAB, 0.7% NaCl) incubated at 65°C for 10 min before protein removal using a conventional phenol-chloroform method (Doyle and Doyle 1987). DNA was precipitated using ethanol at −20°C for 1 h and then resuspended in 50 μL milliq water. DNA integrity was evaluated by agarose gel electrophoresis, quantified using a Quantifluor (Promega) and Quant-iT Picogreen (Invitrogen), and stored at −20°C until further analysis.

For photosynthetic eukaryotes, plastid 16S rRNA gene was amplified using PLA491F forward primer (Fuller *et al.* 2006), which is designed to be biased towards photosynthetic eukaryotes and exclude cyanobacteria, and the oxygenic phototroph reverse primer OXY1313R (West and Scanlan 1999). Amplification was carried out in a total reaction volume of 25 μL containing approximately 5 ng μL^{-1} of community DNA, 200 μM dNTPs, 1.5 mM $MgCl_2$, 1 mg mL^{-1} bovine serum albumin (Promega), 1 μM each primer and 2.5 U Taq polymerase (Promega) in 1× enzyme buffer −Mg (Promega). PCR conditions were as follows: 5 min at 95°C, followed by 30 cycles of 95°C for 30 s, 60°C for 30 s and 72°C for 40 s, with a final extension at 72°C for 6 min. For bacterial analysis, 16S rRNA gene (universal) was amplified using primers 27F and 1492R (Weisburg *et al.* 1991). Amplification was carried out using the same reactants concentration as for photosynthetic eukaryotes. Thermocycler conditions were as follows: 5 min at 94°C, followed by 30 cycles of 94°C for 30 s, 56°C for 30 s and 72°C for 60 s, with a final extension at 72°C for 5 min.

T-RFLP fingerprinting and clone libraries analyses

Plastidial and bacterial 16S rRNA gene fingerprinting analyses were done by terminal restriction fragment length polymorphism (T-RFLP) analysis. For this, primers PLA491F and 27F were labeled at the 5′ end with the 2′-chloro- 5′-fluoro-7′,8′-fused phenyl-1,4-dichloro-6-carboxyfluorescein fluorochrome (NED). Labeled PCR products were overnight digested at 37°C with 20 U of *Hae*III and *Hha*I (plastidial 16S rRNA), and with *Rsa*I and *Hha*I (bacterial 16S rRNA) endonucleases, in a final volume of 20 μL. Each PCR product (in triplicate) was digested separately with each enzyme to assess for T-RFLP profiles consistency. Raw T-RFLP data were handled as previously described (Morán *et al.* 2008).

To identify the community composition by terminal-restriction fragments (T-RFs), two customized databases were generated retrieving sequences from plastidial 16S rRNA and bacterial 16S rRNA genes from NCBI (release February 2013). In addition, a clone library from station Nelson-4 (N4) was constructed from PCR products obtained with primer pair PLA491F/OXY1313 (plastidial 16S rRNA gene), using the TOPO TA Cloning kit (Invitrogen, Life Technologies). Forty-five clones were analyzed and sequenced at Macrogen Inc. (Korea) using M13 forward primer. All sequences were edited by vector removing using Vector NTI 10.3.0. Sequences were compared against published NCBI GenBank database (BLAST 2.2.28+ release February 2013) using blastn (Altschul *et al.* 1990) for initial taxonomical assignation.

454 and Illumina next generation sequencing (NGS) analysis

For photosynthetic eukaryote identification, plastidial 16S rRNA PCR products (in triplicates) were obtained using primer pair PLA491F–OXY1313, purified using Zymoclean kit (Zymo Research) and checked on an Agilent Bioanalzyer DNA1000 chip for the absence of primer dimers, and quantified using a PicoGreen dsDNA quantitation reagent (Invitrogen). Equal amount of purified PCR products were pooled for subsequent 454 pyrosequencing using a Roche GS-FLX Junior. For bacterial identification, general 16S rRNA PCR products (in triplicates) were obtained using primers 515Fseq and 806rcbc (Caporaso *et al.* 2011) following conditions from Earth Microbiome Project (EMP) (Gilbert, Jansson and Knight 2014). Illumina primer constructs were obtained from EMP also. Amplicons were quantified using KAPA Library Quantification Kit (KAPA Biosystem) and sequenced using Illumina Miseq following Caporaso *et al.* (2012) protocol. 12 pM of qPCR quantified amplicons pool were sequenced using a 300 cycles Illumina Miseq kit.

All NGS data analyses were performed using the software package Quantitative Insights Into Microbial Ecology (QIIME, version 1.8 QIIME: http://qiime.org) (Caporaso *et al.* 2010). Sequencing reads were assigned to samples according to their barcodes. Reads with incorrect barcodes, incorrect primer sequences and/or average phred quality score of ≤20 (454 data) and ≤30 (Illumina data) were removed from further analysis.

For 454-based 16S plastidial rRNA gene sequencing, reads were denoised prior to reintegration of the dataset into the QIIME pipeline. Operational taxonomic unit (OTU) picking was performed using an 'open-reference' OTU picking protocol, where sequences are clustered against a specified database and those reads that do not match the reference database are subsequently clustered *de novo*. This step was done using a clusterization at 97% identity using uclust (Edgar 2010). Taxonomic assignments were accomplished using BLAST algorithm (Altschul *et al.* 1990) against PhytoRef database (Decelle *et al.* 2015), with a minimum e-value 1e-5 and 90% identity.

In the case of Illumina 16S rRNA gene sequencing, reads were screened to remove chimeras using usearch61 (Edgar 2010; Edgar *et al.* 2011). OTUs were picked using the 'open-reference' OTU picking strategy, using uclust based on a 97% identity. Taxonomic assignments were done using BLAST algorithm (Altschul *et al.* 1990) with Silva 111 database (Quast *et al.* 2013) (e-value 1e-5 and 90% identity).

To confirm the taxonomical assignation of the 10 most abundant OTUs in each dataset, global alignments against representative sequences were done. Representative sequences were obtained by blastn (Altschul *et al.* 1990) searches against GenBank nr database (release 209, August 2015), excluding taxid: 2 and taxid: 172788, in the case of 454 dataset. In the case of Illumina dataset, searches were against the GenBank 16S ribosomal RNA sequences (Bacteria and Archaea) database (release 209, August 2015), excluding taxid: 56765, 155900 and 77133.

Statistical analysis

Spearman rank correlations were used to explore the relationships between microbial cell counts (PPE, PNE1, PNE2 and total bacteria) and environmental variables (SST, salinity and PAR). T-RFLP fingerprinting profiles were square-root transformed and the data matrices were further analyzed by hierarchical cluster analysis based on Bray–Curtis similarities, using group average as linkage criteria. SIMPROF analysis was used to detect which clusters had non-random structure. Spearman rank correlations were conducted in the R environment version 3.1.1 (R Core Team 2014). Cluster and SIMPROF analyses were conducted using the Primer 6 software (Primer-E, Plymouth, UK). Correlation between both enzymatic T-RFLP profiles for each dataset was checked using the RELATE function in Primer 6 Software.

Multivariate analyses were used to test the prediction of strong relationship between community composition and environmental variation, but weak relationships between community composition and spatial distance (i.e. species-filtering models can explain the variation in microbial community composition in the study site). Because of different numbers of stations available for the three microbial datasets (i.e. cell counts, T-RFLP fingerprinting and NGS analysis), these were analyzed separately and with complementary statistical techniques. Data of cell counts and T-RFLP fingerprints were both sequentially analyzed with permutational multivariate analyses of variance (PERMANOVA) and variance partitioning; data of NGS were analyzed with procrustes analyses. These analyses were conducted in the R environment version 3.1.1 (R Core Team 2014).

We used PERMANOVA (Anderson 2001), based on Euclidean distances, to analyze the spatial variability in community composition according to the position of the sampling stations relative to nearest glaciers, according to our previous categorization (see Table 1). Euclidean distances were used here to avoid the estimation of zero variances. Then, a one-way PERMANOVA with 'zone' as fixed factor was conducted on standardized cell counts and T-RFLP data. Homogeneity of multivariate dispersion was corroborated with PERMDISP analyses after each PERMANOVA.

Variation partitioning analyses, based on redundancy analyses (RDA), were used to separate the variation of photosynthetic eukaryote and heterotrophic bacteria microbial communities with respect of the environmental parameters and spatial distance. Before the analyses, abundance and environmental data were standardized to zero mean and variance unit. The spatial distances among sampling stations were calculated from latitude–longitude data. The spatial distances were transformed to rectangular principal coordinates of neighborhood matrices (PCNM) in order to be used in the variance partitioning analyses (Borcard 2002). PCs from each neighborhood matrix were selected according to the Akaike information criterion (AIC) values after stepwise model building—models scoring the lowest AIC values were selected. Then, the fractions of variation in the biotic abundance data accounted for by the spatial distance at different scales (selected PCNM), and the matrix of environmental factors was estimated as adjusted R^2 from RDA (constrained) ordinations. The significance of each model was estimated by means of 1000 permutations.

For the NGS dataset, procrustes analyses were conducted to estimate the concordance of site scores in constrained (RDA including the environmental factors) and unconstrained (principal components analysis) analyses of the abundance data. The statistical significance of the correlation between ordinations was tested by means of 1000 permutations. A significant correlation between constrained and unconstrained ordinations was used as evidence that the measured environmental variables accounted for most of the biological variation (Ramette and Tiedje 2007), providing support for the species-filtering model.

Nucleotide sequence accession numbers

Clone libraries nucleotide sequences have been deposited under GenBank accession numbers KT956274 to KT956318. 454 and Illumina nucleotide sequences have been deposited in Sequence Read Archive under BioProject number PRJNA280421.

RESULTS

Oceanographic context of Fildes Bay, King George Island, Antarctica

During the sampling period, surface waters from Fildes Bay were characterized by heterogeneous hydrographic conditions (Fig. 2a). In general, saltier (≥33.8 psu), denser (>27 kg m^{-3}) and relatively warmer (>2°C) waters were found at stations located at Collins Bay (C1–C3), in comparison to those located at Fildes peninsula (F1, F2 and F4), Nelson Island (N1-N3) and Fildes Bay mouth (IB1 and IB2) (Fig. 1). Waters with the lowest density (<27 kg m^{-3}) were observed at station C4, and in a less degree at the inner bay station IB3, likely due to the influence of freshwater coming from the Marian Cove. The inner part of Edgell Bay (station N4) showed a noteworthy rise in temperature (up to 2.75°C), which determined a clear drop in density. The coastal station closer to Fildes Ice Cap (F3) showed colder (1.7°C), saltiest

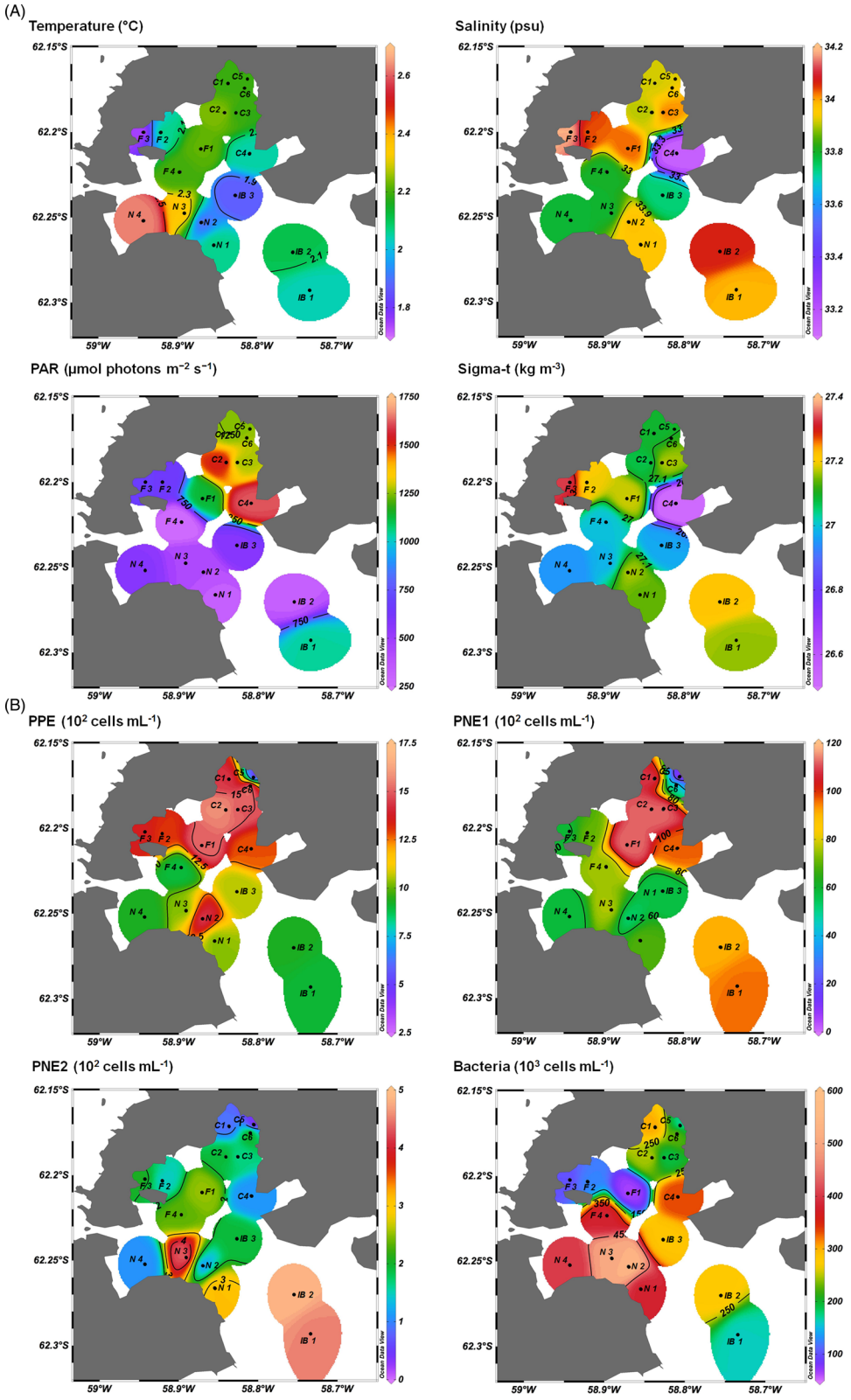

Figure 2. Physical data (temperature, salinity, PAR, sigma t) (**A**) and photosynthetic eukaryotes and bacterial cell counts (**B**) at 5 m depth at Fildes Bay, King George Island, West Antarctic Peninsula. PPE: photosynthetic picoeukaryotes; PNE1: photosynthetic nanoeukaryotes group 1; PNE2: photosynthetic nanoeukaryotes group 2.

Table 2. Spearman correlation matrix for bacteria and phytoplankton groups abundances vs physical variables.

	PPE[a]	PNE1[b]	PNE2[c]	Bacteria	Salinity	SST
PPE						
PNE1	0.40					
PNE2	− 0.55	− 0.01				
Bacteria	− 0.43	− 0.39	− 0.15			
Salinity	− 0.16	− 0.55	0.23	− 0.14		
SST	− 0.18	0.49	0.38	− 0.02	− 0.73**	
PAR	0.80**	0.75**	− 0.44	− 0.57*	− 0.40	0.14

[a]PPE, photosynthetic picoeukaryotes; [b]PNE1, photosynthetic nanoeukaryotes group 1; [c]PNE2, photosynthetic nanoeukaryotes group 2. $P < 0.1$, *$P < 0.05$, **$P < 0.01$.

(34.2 psu) and denser (27.3 kg m^{-3}) waters. A marked gradient in PAR was found, decreasing from northeastern to western (F1–F4) and southern (N1–N3 and IB2–IB3) stations. PAR increased again to the most outer station (IB1). A more complex pattern was observed through the water column, with a marked stratification due to influence of deep waters. In general, relative warmer waters at surface changed to cooler, salty and denser waters in a steep gradient at depths that change in an opposite way with the bathymetry (see Fig. S1, Supporting Information).

Photosynthetic eukaryotes and bacterial cell counts

Three different photosynthetic eukaryotes groups were detected according to their optical properties measured by flow cytometry (FCM). These particles differ in time pulse width and forward angle light scattering (FSCperp) (Fig. S2a, Supporting Information), parameters that were recently used as proxies of particles shape and size (Hoffman 2009). The most abundant group, defined as photosynthetic nanoeukaryotes (PNE1), showed intermediate FSCperp, pulse width and red fluorescence, with cell counts values ranging from 2.5 to 112.8 × 10^2 cells mL^{-1}, this group was followed by a group of particles with lower levels of these three parameters, defined as photosynthetic picoeukaryotes. They display an order of magnitude less abundance, ranging from 3.2 to 17.4 × 10^2 cells mL^{-1} (Table 1). The third group detected, defined also as photosynthetic nanoeukaryote (PNE2), showed higher levels of the optical properties, and was considerably less abundant than PNE1 and PPE. No orange fluorescence (a proxy for cyanobacteria) was detected (Fig. S2b, Supporting Information). Total bacterial cell counts were three orders of magnitude higher than eukaryotic phytoplankton, with values ranging from 65.4 × 10^3 to 554 × 10^3 cells mL^{-1} (Table 1).

The groups described above showed differing spatial patterns. For example, PNE1 and PPE were mostly concentrated in stations located near Collins Glacier (Fig. 2b). PNE2, on the other hand, showed the highest cell concentrations (4.2–4.9 × 10^2 cells mL^{-1}) in stations located in the mouth of the bay (i.e. stations IB1 and IB2 in Fig. 1). Bacteria peaked near Nelson Glacier. Spearman correlations showed that PNE1 and PPE cell counts were positively correlated with PAR (Fig. 2 and Table 2). On the other hand, bacterial cell counts were negatively correlated with PAR (Fig. 2 and Table 2). PNE2 showed weak and non-significant correlations with environmental variables. Salinity was negatively and significantly correlated with SST (Table 2). Therefore, salinity was removed from further multivariate analyses in order to reduce colinearity. PERMANOVA showed differing multivariate patterns between photosynthetic eukaryotes and bacterial cell abundances: while the photosynthetic eukaryote groups showed no significant relationship with sampling zone (pseudo-$F_{3,13} = 1.13$, $P > 0.05$), the bacteria did (pseudo-$F_{3,13} = 1.95$, $P = 0.03$); these differences were due to differences in the location of group centroids and not in dispersion (PERMDISP, $P > 0.05$ for both groups).

Variation partition analyses showed that the variation in photosynthetic eukaryote abundances was mostly accounted for by the spatial factors in comparison with the environmental factors (ca. 41% and 31%, respectively). On the contrary, the variation in bacterial abundances was mostly accounted for by the environmental factors (ca. 35% and 4% for environmental and spatial factors, respectively). Both, the spatial and environmental fractions were statistically significant for photosynthetic eukaryotes and bacteria ($P < 0.01$). The joint contribution of environmental and spatial factors accounted for ca. 5% and 4% of the variation in community cell counts of photosynthetic eukaryote and bacterial communities, respectively.

T-RFLP fingerprinting of microbial communities

T-RFLP fingerprinting analysis of 16S rRNA marker genes for photosynthetic eukaryotes and bacterial communities showed a high degree of correlation (Spearman rank correlation, $r_s = 0.30$, $P < 0.01$; and $r_s = 0.70$, $P < 0.01$, respectively) between pairs of restriction enzymes used in each group of organisms (*Hae*III and *Hha*I; *Rsa*I and *Hha*I, respectively). T-RFLP profiles of photosynthetic eukaryote communities revealed between 6 and 19 consistent T-RFs across stations. Cluster analysis based on Bray–Curtis resemblances revealed two main groups of samples: one composed by samples from stations closer to the Collins Glacier and Fildes area, and another group composed by a combination of stations from the four zones (Fig. 3a). On the other hand, PERMANOVA showed no statistical differences in the composition of photosynthetic eukaryotes communities among Collins, Nelson, Inner Bay and Fildes zones in terms of centroid locations (pseudo-$F_{3,13} = 0.99$, $P > 0.05$) and multivariate dispersion ($P > 0.45$). Moreover, variance partitioning showed negligible fractions of variance in community composition accounted for by the environmental (ca. 7%, $P > 0.05$) and spatial (ca. 2%, $P > 0.05$) factors. The interaction between environment and space accounted for ca. 3% and the residual for 88% of the total variation in photosynthetic eukaryotes.

In the case of bacterial community composition, T-RFLP analysis indicated the presence of between 5 and 21 consistent T-RFs. Cluster analysis based on Bray–Curtis dissimilarity reveal three marked groups (Fig. 3b). We observed significant differences among zones within the bay in terms of centroid locations (pseudo-$F_{3,10} = 1.84$, $P = 0.02$), but not in terms of multivariate dispersion ($P > 0.05$). The environmental and spatial factors accounted for ca. 20% ($P = 0.01$) and 11% ($P = 0.02$) of the multivariate composition of bacterial communities; the joint influence of both matrices was negligible (ca. 0%) and the residual variation accounted for 74%.

In silico restriction analysis of a customized database including the plastidial 16S rRNA gene clone library (Table S1, Supporting Information) indicated that main T-RFs might corresponded to *Thalassiosira*- and *Phaeocystis*- like sequences, with 46 ± 7% and 27 ± 7% (mean ± SD) of relative abundance. Other important groups were Prasinophyceae-like sequences (see Fig. 3a). The same analysis for bacterial 16S rRNA, but considering only public sequences (Table S2, Supporting Information), showed a high dominance of Proteobacteria, particularly an OTU closely related to Deltaproteobacteria class, with 30 ± 10% relative

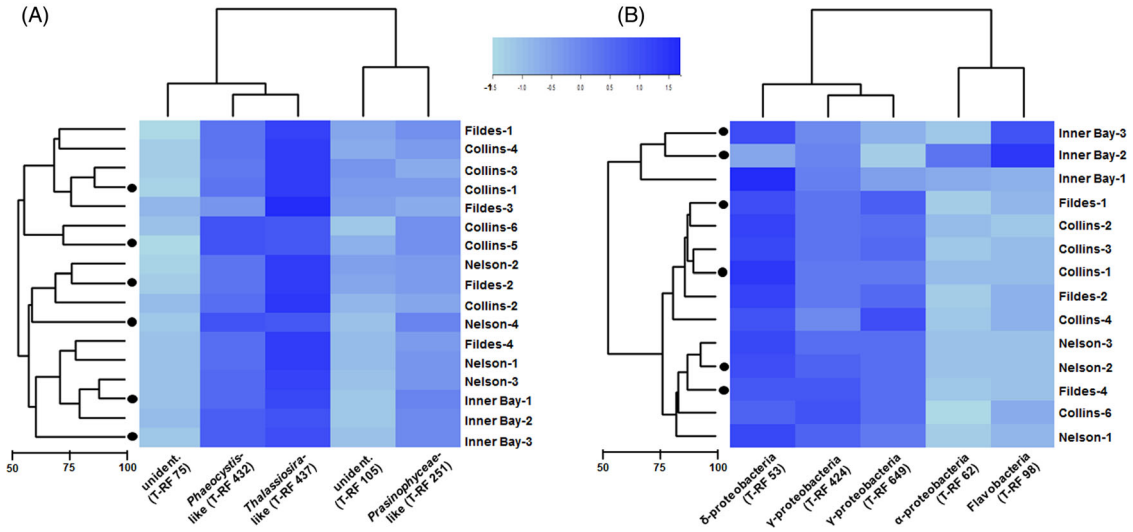

Figure 3. Dendograms of hierarchical cluster analyses based on Bray–Curtis similarities comparing photosynthetic eukaryotes (**A**) and bacterial (**B**) T-RFLP patterns in each sampling station. Heatmaps represent relative abundance of the five dominant T-RFs in each microbial component. Heatmap scale corresponds to log relative abundance of each T-RF. Black dots denote selected samples for NGS.

abundance, followed by an OTU closely related to Gammaproteobacteria class (relative abundance of 17 ± 5%, mean ± SD), and Flavobacteria class (7 ± 14%).

Community composition determined by NGS

Detailed taxonomic characterization of the microbial communities in Fildes Bay was accomplished using NGS of six samples that were selected based on T-RFLP supported clusters (SIMPROF analysis for photosynthetic eukaryotes Pi = 1.62, $P = 0.001$; for Bacteria Pi = 8.99, $P = 0.001$) (see Fig. 3). An overview of sequencing datasets is provided in Table 3. For photosynthetic eukaryotes analysis, plastidial 16S rRNA gene high-throughput sequencing produced 14 706 high quality and denoised reads. These sequences were clustered at a similarity threshold of 97% into 175 OTUs. Bacterial 16S rRNA gene sequencing produced 5 731 111 reads and 17 846 OTUs, after clustering at 97% similarity. Plastidial and cyanobacterial sequences accounted for 30 ± 18% and 2.5 ± 0.5% (mean ± SD) of relative abundance, respectively, and were not considered for further analysis. Rarefaction curves constructed using the chao-1 richness estimator indicated a deep coverage in all stations analyzed (Fig. S3, Supporting Information).

In agreement with T-RFLP data, community composition analysis using NGS indicated that photosynthetic eukaryote communities were highly similar across stations (>85% Bray–Curtis similarities from raw data), and dominated at the supergroup level by Stramenopiles and Haptophytes, with relative abundances of 60 ± 12% and 29 ± 9%, respectively. Additionally, Apicomplexa (5 ± 3%) and Cryptophytes (2 ± 1%) assigned sequences were also detected (Fig. 4a). Within the Stramenopiles, most sequences were assigned to Diatoms groups (Stephanodiscaceae, *Chaetoceros*, Thalassiosirales, *Fragilariopsis* and Bacillariophyceae), while haptophytes sequences were assigned to Chrysochromulinaceae and Phaeocystaceae. Within the cryptophytes, Pyrenomonadales assigned sequences were also important in abundance. Local alignments of the 10 most abundant photosynthetic eukaryote OTUs representing 70 ± 9.4% (mean ± SD) relative abundance (Table S3, Supporting Information) confirmed their taxonomic assignation. These eukaryotic organisms were also the most T-RFs representatives. The procrustes matrix-rotation analysis showed a non-significant correlation between the constrained (i.e. RDA including the environmental factors) and the unconstrained ordinations (Pearson product moment, $r = 0.57$, $P > 0.05$), suggesting that environmental factors did not account for a significant fraction of the

Table 3. Overview of the NGS datasets.

454 data			Illumina data		
Sample	HQ reads[a]	Number of rep. OTUs	Sample	HQ reads[b]	Number of rep. OTUs
C1	1975	21	C1	1285 932	5083
C5	3639	38	F1	1076 678	3713
F2	3911	50	IB2	667 537	1776
IB1	1537	19	IB3	795 717	2292
IB3	916	6	N2	1148 607	2846
N4	2728	41	N4	756 640	2136
Total	14 706	175	Total	5731 111	17 846

[a]Correspond to high quality and denoised reads; [b]Correspond to high quality and unchimeric reads.

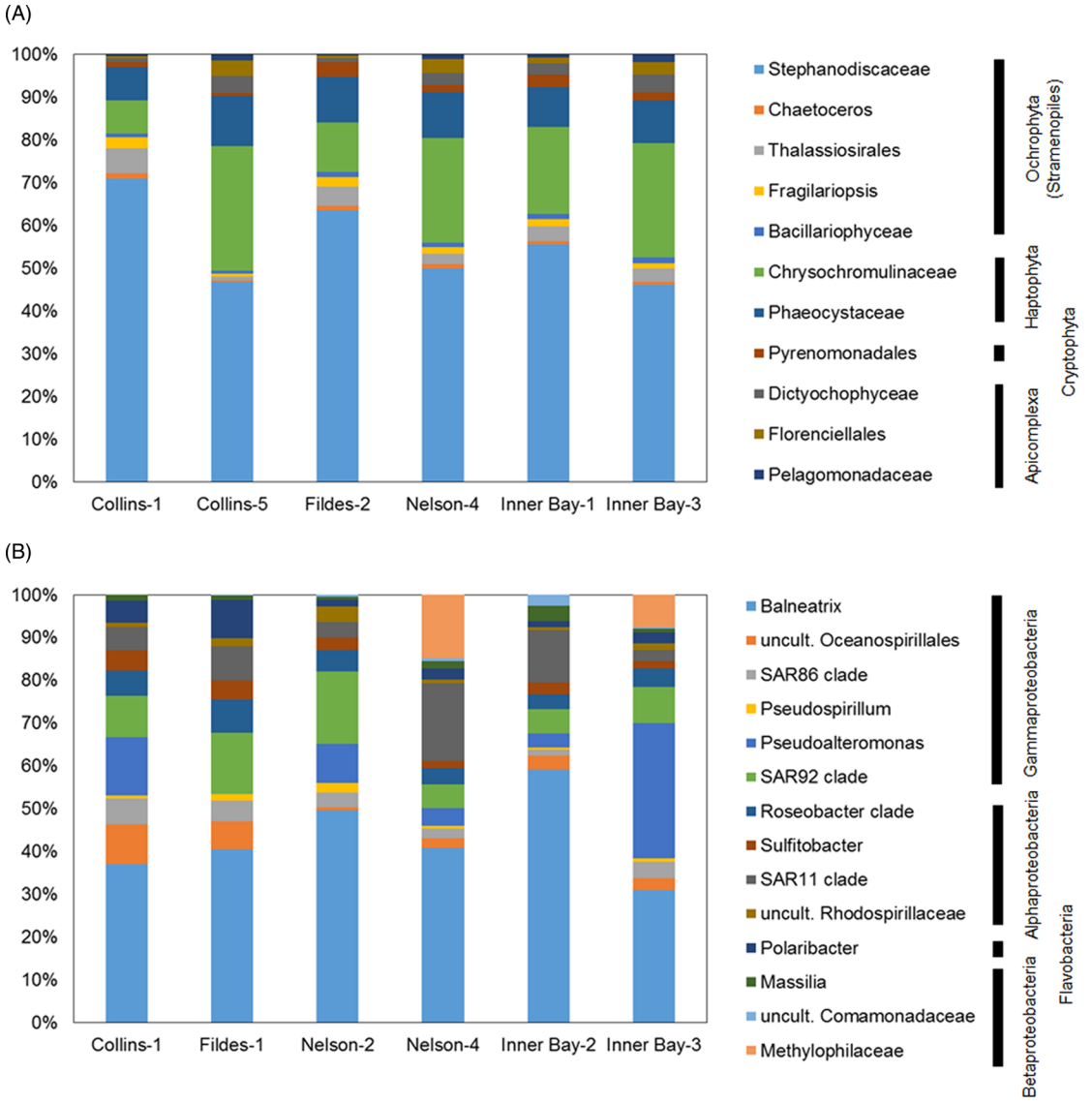

Figure 4. Taxonomic distribution of photosynthetic eukaryotes (**A**) and bacterial (**B**) communities at selected stations inside Fildes Bay. Relative abundance of sequences was calculated based on NGS of plastidial (A) or bacterial (B) 16S rRNA gene. Only groups with a relative abundance above 0.1% are shown.

multivariate composition of photosynthetic eukaryotes determined by means of NGS.

In the case of bacteria, community compositions determined by NGS were >75% similar based on Bray–Curtis similarities (calculated from raw data). Taxonomic identification was consistent with T-RFLP data, and indicates a dominance of Gammaproteobacteria (40 ± 16% relative abundance mean and SD), followed by Alphaproteobacteria (9 ± 2%), Betaproteobacteria (3 ± 2%) and Flavobacteria (2 ± 1%) (Fig. 4b). Most abundant taxa included members of the order Oceanospirillales (Gammaproteobacteria), with a dominance of *Balneatrix* assigned sequences, followed by *Pseudoalteromonas*. Local alignments of the 10 most abundant bacterial OTUs (representing 52 ± 7.1% relative abundance; Table S4, Supporting Information) confirmed their taxonomic assignation. In agreement with our previous analysis of bacterial communities examined with T-RFLP, the procrustes analysis of NGS data showed a significant and tight correlation between the constrained and unconstrained ordinations (Pearson product moment, $r = 0.92$, $P < 0.01$), suggesting that most of the variation in this assemblage was accounted for by differences in environmental conditions.

DISCUSSION

In this study, microbial communities in an Antarctic coastal system were analyzed to reveal the influence of environmental filtering and spatial distances over cellular abundances and community composition at the local scale. Two key microbial components of the Antarctic marine ecosystem were contrasted: photosynthetic microbial eukaryotes, known for being the primary food source for Antarctic marine trophic networks (Smetacek and Nicol 2005; Browning *et al.* 2014) and bacteria, one of the main contributors to energy fluxes into the microbial food webs through heterotrophy and the microbial loop (Azam *et al.* 1983; Cole, Findlay and Pace 1988; Ducklow 2000). Results presented here indicate that, at submesoscale, environmental filtering seems to control the spatial variation of these communities. However, the degree to which environmental

filters accounted for community-level spatial variation differed between microbial components: while photosynthetic microbial eukaryotes showed weak or non-existent influence of environmental filtering on cellular abundance and community composition, environmental parameters strongly affected both attributes of bacterial communities. In addition, the high influence of environmental factors (independent of space) suggests that these factors are major drives of bacterial community structure. In order to explain these patterns, on the following lines we provide testable working hypotheses that would stimulate further experimental work in this fragile and still poorly explored marine ecosystem.

Oceanographic context and environmental gradients at submesoscale in Fildes Bay, King George Island, Antarctica

During the sampling period (beginning of January 2012), the composition of the water column at Fildes Bay was strongly influenced by less saline waters near the Collins Glacier area due to freshwater melting, and by low PAR values near Nelson Island, likely due to the high amount of particulate material derived from marine bird settlements. The influence of glacier melting on the water column structure is a well-documented phenomenon (Piquet *et al.* 2011), which has been shown to be involved in water column stratification and to favor the development of some phytoplanktonic and bacterial groups (Piquet *et al.* 2014; Gutiérrez *et al.* 2015). Besides, similar hydrographic characteristics have been previously reported at Fildes Bay (Chang *et al.* 1990), indicating that the observed structure is a recurrent pattern. These results suggest that Fildes Bay presents strong environmental gradients over small spatial distances, and that these gradients are the result of the characteristics of surrounding areas. In this way, further long-term environmental data should be analyzed in order to test this hypothesis.

Environmental filtering and photosynthetic eukaryotes communities

The variation in the photosynthetic eukaryote communities was mainly accounted for by spatial distance, with a significant influence over cellular abundances but not for taxonomic composition. Both cell abundances and taxonomic composition showed weak or non-significant relation with sampling zone or environmental parameters, with the exception of PAR. A strong correlation between PAR availability and phytoplankton cell abundances is expected due to the photosynthetic requirements of this group of organisms, although differences have been observed between functional groups and size classes as well (Cherrier *et al.* 2015; Edwards *et al.* 2015). Specifically, diatoms and haptophytes, such as the genus *Phaeocystis*, have been shown to be most responsive photosynthetic group to light increases (Edwards *et al.* 2015). Our results contrast with previous studies (Olsen *et al.* 2013) in which a strong effect of environmental filtering over phytoplankton community composition was detected in surface waters around the South Shetland Island, but at a higher scale, with distance between stations >50 km. Collectively, these data suggest that eukaryotic phytoplankton respond to broader differences in environmental variables (Olsen *et al.* 2013), but at short scales tend to display homogeneous patterns (this study). Recently, a global-scale survey indicated that geographic distance has an influence on defining microbial community composition, but with a higher impact as cellular size increases (De Vargas *et al.* 2015). Unfortunately, this last study did not include the analysis of the bacterial compartment.

The photosynthetic eukaryote community from Fildes Bay was dominated by nanoplanktonic cells, as opposed to the dominance of picoeukaryotes reported in other Polar regions such as the Arctic coastal zone of Beaufort Sea, in which PPE were around 11–1300 cell mL^{-2} (Balzano *et al.* 2012). It has been proposed that high nutrient status favors the dominance of larger cells, outcompeting the pico-sized fraction (Barber and Hiscock 2006). Even when for this study was not possible to obtain nutrient measurements due to logistics constrains, factors producing high nutrient concentrations, such as heavy metal pollution (Santos *et al.* 2005), high amount of decomposition of macroalgae (Nedzarek 2004), penguin rookeries (Juchnowicz-Bierbasz and Rakusa-Suszczewski 2002) and glacier melting with the consequent remineralization of inorganic nutrients (Dawson, Schramm and Bölter 1985), have been reported for coastal zones of King George Island. In agreement with FCM cell count analyses, photosynthetic eukaryote communities were dominated by sequences related to nano-sized cell organisms. *Thalassiosira*-like sequences were the most abundant T-RFs retrieved in our fingerprinting profiles and a more detailed taxonomic affiliation obtained by NGS reveals a high dominance of *Stephanodiscus* sequences, a diatom closely related to *Thalassiosira*. The second most dominant group retrieved by T-RFLP and NGS was the haptophyte *Phaeocystis*. The dominance of these two nanoplanktonic organisms in Antarctic waters has been previously reported by light microscopy, pigment-based and molecular approaches (Weber and El-Sayed 1987; Piquet *et al.* 2008; Mendes *et al.* 2012).

Environmental filtering and bacterial communities

Bacterial cell numbers at Fildes Bay ranged between 65 and 553 cells mL^{-3}, spanning an order of magnitude in abundance levels with a clear increase toward Nelson Island. The areas surrounding Nelson Glacier showed lower availability of PAR than in other stations, attributable to water turbidity caused by dense marine bird settlements nearby. It has been shown that fecal material from penguins and other marine birds can influence light availability due to the increase in particulate material (Jauffrais *et al.* 2015). In agreement with the FCM cell counts analysis, T-RFLP data showed the presence of three different clusters, one conformed by samples mostly belonging to Nelson Island with a high dominance of Gammaproteobacteria, a group known to harbor particle-attached representatives (Crespo *et al.* 2013). Moreover, the role of bacteria in the decomposition of penguin guano has been described for intertidal bacteria in Admiralty Bay (Zdanowski, Zmuda and Zwolska 2005), and the same metabolic behavior can be expected for marine bacteria at Fildes Bay. Besides, bacteria have shown to display a wide range of responses to available PAR, with taxa-specific responses. Available evidence suggests that increases in PAR and UVR exert a significant effect on heterotrophic bacterial populations (reviewed in Ruiz-González *et al.* 2013), with strong inhibition of bacterial activities in some cases. However, the knowledge about how PAR affects heterotrophic bacteria abundances and compositions is still in early development, and could be a relevant topic of future research in Antarctic environments, where increases in PAR and UV radiation are predicted as a consequence of ongoing global changes (Turner *et al.* 2005).

NGS allowed us to accurately confirm the dominance of Gammaproteobacteria sequences, specifically the Oceanospirillales member *Balneatrix*. Evidence for *Balneatrix* as an important

member of the bacterial West Antarctic Peninsula water community has been recently reported (Nikrad, Cottrell and Kirchman 2013; Zeng *et al.* 2013), highlighting its relevance as a cosmopolitan member of coastal Antarctic bacterial communities. However, to date, no information about the metabolisms of this Antarctic-ubiquitous taxon has been reported.

Variation in community composition of bacterial component was strongly influenced by environmental filtering. Both cellular abundances and taxonomic profiles were clearly determined by environmental variation, with strong differences in abundances and composition through Nelson Zone. Moreover, the fact that the 'pure' effects of environmental factors were comparatively high than their joint effects with space strongly indicates that environmental filters constitute an important driver of bacterial community structure. Same as for phytoplankton, this results contrast with previous data for the same region obtained by DGGE fingerprinting analysis (Olsen *et al.* 2013). However, differences in sampling scale and resolution of taxonomic assignations should be taken into account when comparing both studies. In our study, two different high-throughput sequence technologies were applied to unveil microbial taxonomic composition. Even when an inherent difference between the two technologies is expected (i.e. Illumina runs give hundreds time more sequence data than 454), both groups of libraries gave us excellent coverages of the microbial diversity, as observed on the rarefaction analysis. In addition, the high concordance between fingerprinting and NGS approach gives further support to the observed patterns in our study. The use of multivariate variance-partitioning approaches for hypothesis testing based on the combination of molecular approaches has shown to be a powerful tool to access microbial ecological patterns with high taxonomic resolution (e.g. Winter, Matthews and Suttle 2013).

CONCLUSION

In conclusion, our correlative results supported the general hypothesis of environmental controls on microbial communities in Fildes Bay, Antarctica. However, the strength of these controls differed markedly between photosynthetic eukaryotes and bacterial communities, with nil environmental responses of former but strong and significant responses of the latter. The comparison of our results with previous records suggests that photosynthetic assemblages respond stronger to broad scale rather than fine-scale environmental variability. On the other hand, the metabolic versatility of bacteria may give them the ability to respond promptly to fine-scale environmental changes, increasing in cell densities of specific groups. With these hypotheses, we hope to stimulate further observational and manipulative research on the role of environmental filtering in structuring the microbial communities in the threatened, but yet not well-understood Antarctic marine ecosystems.

SUPPLEMENTARY DATA

Supplementary data are available at FEMSEC online.

ACKNOWLEDGEMENTS

We thank the staff at 'Prof. Julio Escudero' INACH Research Station for logistic support, and Carolina Sánchez and Marcela Astete from the Sequencing core at UMayor. We also would like to thanks Marcelo Rojas-Herrera for bioinformatic technical help.

FUNDING

This work was supported by Instituto Antártico Chileno (INACH) Grant T16-10 and Fondo Nacional de Desarrollo Científico y Tecnológico (FONDECYT) Grant # 11121554. NV was supported by FONDECYT grant # 1141037 and Programa de Investigación Asociativa (PIA) Anillo grant ART1101 and FONDAP-IDEAL grant # 15150003.

Conflict of interest. None declared.

REFERENCES

Altschul SF, Gish W, Miller W *et al.* Basic local alignment search tool. *J Mol Biol* 1990;**215**:403–10.

Anderson MJ. A new method for non parametric multivariate analysis of variance. *Austral Ecol* 2001;**26**:32–46.

Ardyna M, Gosselin M, Michel C *et al.* Environmental forcing of phytoplankton community structure and function in the Canadian High arctic: contrasting oligotrophic and eutrophic regions. *Mar Ecol Prog Ser* 2011;**442**:37–57.

Arrigo KR, Robinson D, Worthen DL *et al.* Phytoplankton community structure and the drawdown of nutrients and CO2 in the southern ocean. *Science* 1999;**283**:365–7.

Azam F, Fenchel T, Field JG *et al.* The ecological role of water-column microbes in the sea. *Mar Ecol Prog Ser* 1983;**10**:257–64.

Azam F, Malfatti F. Microbial structuring of marine ecosystems. *Nat Rev Microbiol* 2007;**5**:782–91.

Azam F, Worden AZ. Oceanography. Microbes, molecules, and marine ecosystems. *Science* 2004;**303**:1622–4.

Baas Becking LGM. *Geobiologie of Inleiding tot de Milieukunde*. The Hague, The Netherlands: W.P. Van Stockum, Zoon, 1934.

Balzano S, Marie D, Gourvil P *et al.* Composition of the summer photosynthetic pico and nanoplankton communities in the Beaufort Sea assessed by T-RFLP and sequences of the 18S rRNA gene from flow cytometry sorted samples. *ISME J* 2012;**6**:1480–98.

Barber RT, Hiscock MR. A rising tide lifts all phytoplankton: growth response of other phytoplankton taxa in diatom-dominated blooms. *Global Biogeochem Cy* 2006;**20**:1–12.

Behrenfeld MJ, Randerson JT, McClain CR *et al.* Biospheric primary production during an ENSO transition. *Science* 2001;**291**:2594–7.

Borcard D, Legendre P. All-scale spatial analysis of ecological data by means of principal coordinates of neighbour matrices. *Ecol Model* 2002;**153**:51–68.

Browning TJ, Bouman HA, Moore CM *et al.* Nutrient regimes control phytoplankton ecophysiology in the South Atlantic. *Biogeosciences* 2014;**11**:463–79.

Caporaso JG, Kuczynski J, Stombaugh J *et al.* Correspondence QIIME allows analysis of high- throughput community sequencing data Intensity normalization improves color calling in SOLiD sequencing. *Nat Publ Gr* 2010;**7**:335–6.

Caporaso JG, Lauber CL, Walters W *et al.* Global patterns of 16S rRNA diversity at a depth of millions of sequences per sample. *P Natl Acad Sci USA* 2011;**108**:4516–22.

Caporaso JG, Lauber CL, Walters WA *et al.* Ultra-high-throughput microbial community analysis on the Illumina HiSeq and MiSeq platforms. *ISME J* 2012;**6**:1621–4.

Crespo BG, Pommier T, Fernández-Gómez B *et al.* Taxonomic composition of the particle-attached and free-living bacterial assemblages in the Northwest Mediterranean Sea analyzed by pyrosequencing of the 16S rRNA. *MicrobiologyOpen* 2013;**2**:541–52.

Chang KI, Jun HK, Park GT *et al.* Oceanographic conditions of Maxwell Bay, King George Island, Antarctica (Austral summer 1989). *Korean J Polar Res* 1990;**1**:27–46.

Cherrier J, Valentine S, Hamill B *et al.* Light-mediated release of dissolved organic carbon by phytoplankton. *J Mar Syst* 2015;**147**:45–51.

Clarke A, Murphy EJ, Meredith MP *et al.* Climate change and the marine ecosystem of the western Antarctic Peninsula. *Philos T Roy Soc B* 2007;**362**:149–66.

Cole J, Findlay S, Pace M. Bacterial production in fresh and saltwater ecosystems: a cross-system overview . *Mar Ecol Prog Ser* 1988;**43**:1–10.

Dawson R, Schramm W, Bölter M. Factors influencing the production, decomposition and distribution of organic and inorganic matter in Admiralty Bay, King George island. In Siegfried WR, Condy PR, Laws RM, (eds). *Antarctic Nutrient Cycles and Food Webs*. 1985, 109–14.

Decelle J, Romac S, Stern RF *et al.* PhytoREF: a reference database of the plastidial 16S rRNA gene of photosynthetic eukaryotes with curated taxonomy. *Mol Ecol Resour* 2015;**15**: 1435–45.

De La Iglesia R, Trefault N. Marine photosynthetic eukaryotes in polar systems: unveiling phytoplankton diversity and composition in Antarctic waters. *Rev Chil Hist Nat* 2012;**85**:435–43.

de Vargas C, Audic S, Henry N *et al.* Eukaryotic plankton diversity in the sunlit ocean. *Science* 2015;**348**:1–10.

Dierssen HM, Smith RC, Vernet M. Glacial meltwater dynamics in coastal waters west of the Antarctic peninsula. *P Natl Acad Sci USA* 2002;**99**:1790–5.

Díez B, Massana R, Estrada M *et al.* Distribution of eukaryotic picoplankton assemblages across hydrographic fronts in the Southern Ocean, studied by denaturing gradient gel electrophoresis. *Limnol Oceanogr* 2004;**49**:1022–34.

Doyle JJ, Doyle JL. A rapid DNA isolation procedure for small quantities of fresh leaf tissue. *Phytochem Bull* 1987;**19**:11–5.

Ducklow H. Bacterial production and biomass in the oceans. *Microb Ecol Oceans* 2000;**1**:85–120.

Edgar RC. Search and clustering orders of magnitude faster than BLAST. *Bioinformatics* 2010;**26**:2460–1.

Edgar RC, Haas BJ, Clemente JC *et al.* UCHIME improves sensitivity and speed of chimera detection. *Bioinformatics* 2011; **27**:2194–200.

Edwards KF, Thomas MK, Klausmeier CA *et al.* Light and growth in marine phytoplankton: allometric, taxonomic, and environmental variation. *Limnol Oceanogr* 2015;**60**:540–52.

Falkowski PG, Fenchel T, Delong EF. The microbial engines that drive Earth's biogeochemical cycles. *Science* 2008;**320**: 1034–9.

Fuller NJ, Campbell C, Allen DJ *et al.* Analysis of photosynthetic picoeukaryote diversity at open ocean sites in the Arabian Sea using a PCR biased towards marine algal plastids. *Aquat Microb Ecol* 2006;**43**:79–93.

Ghiglione J-F, Galand PE, Pommier T *et al.* Pole-to-pole biogeography of surface and deep marine bacterial communities. *P Natl Acad Sci USA* 2012;**109**:17633–8.

Gilbert JA, Jansson JK, Knight R. The Earth Microbiome project: successes and aspirations. *BMC Biol* 2014;**12**:69.

Grzymski JJ, Riesenfeld CS, Williams TJ *et al.* A metagenomic assessment of winter and summer bacterioplankton from Antarctica Peninsula coastal surface waters. *ISME J* 2012;**6**:1901–15.

Gutiérrez M, Galand P, Moffat C *et al.* Melting glacier impacts community structure of Bacteria, Archaea and Fungi in a Chilean Patagonia fjord. *Environ Microbial* 2015;**17**:3882–97.

Hanson CA, Fuhrman JA, Horner-Devine MC *et al.* Beyond biogeographic patterns: processes shaping the microbial landscape. *Nat Rev Microbiol* 2012;**10**:497–506.

Holyoak M, Leibold MA, Holt RD. *Metacommunities: Spatial Dynamics and Ecological Communities*. Chicago: University of Chicago Press, 2005.

Hoffman RA. Pulse width for particle sizing. *Curr Protoc Cytom* 2009, 1–17.

Jauffrais T, Drouet S, Turpin V *et al.* Growth and biochemical composition of a microphytobenthic diatom (Entomoneis paludosa) exposed to shorebird (Calidris alpina) droppings. *J Exp Mar Bio Ecol* 2015;**469**:83–92.

Jiang Y, Yang EJ, Kim SY *et al.* Spatial patterns in pelagic ciliate community responses to various habitats in the Amundsen Sea (Antarctica). *Prog Oceanogr* 2014;**128**:49–59.

Juchnowicz-Bierbasz M, Rakusa-Suszczewski S. Nutrients and cations in soil solution from the present and relict penguin colonies (Admiralty Bay, King George Island). *Pol J Ecol* 2002;**50**:79–91.

Karl D, Proctor L. Foundations of microbial oceanography. *Oceanography* 2007;**20**:16–27.

Lee SH, Dahms HU, Kim Y *et al.* Spatial distribution of small phytoplankton composition in the Chukchi Sea. *Polar Biol* 2014;**37**:99–109.

Logue JB, Mouquet N, Peter H *et al.* Empirical approaches to metacommunities: a review and comparison with theory. *Trends Ecol Evol* 2011;**26**:482–91.

López-García P, Rodríguez-Valera F, Pedrós-Alió C *et al.* Unexpected diversity of small eukaryotes in deep-sea Antarctic plankton. *Nature* 2001;**409**:603–7.

Luria C, Ducklow H, Amaral-Zettler L. Marine bacterial, archaeal and eukaryotic diversity and community structure on the continental shelf of the western Antarctic Peninsula. *Aquat Microb Ecol* 2014;**73**:107–21.

Martins CC, Bícego MC, Taniguchi S *et al.* Aliphatic and polycyclic aromatic hydrocarbons in surface sediments in Admiralty Bay, King George Island, Antarctica. *Antarct Sci* 2004;**16**: 117–22.

Mendes CRB, de Souza MS, Garcia VMT *et al.* Dynamics of phytoplankton communities during late summer around the tip of the Antarctic Peninsula. *Deep-Sea Res Pt I* 2012;**65**: 1–14.

Mohapatra BR, Rellinger AN, Kieber DJ *et al.* Comparative functional characteristics of DMSP lyases extracted from polar and temperate Phaeocystis species. *Aquat Biol* 2013;**18**: 185–95.

Monier A, Comte J, Babin M *et al.* Oceanographic structure drives the assembly processes of microbial eukaryotic communities. *ISME J* 2014;**9**:990–1002.

Morán AC, Hengst MB, De la Iglesia R *et al.* Changes in bacterial community structure associated with coastal copper enrichment. *Environ Toxicol Chem* 2008;**27**:2239–45.

Nedzarek A, Rakusa-Suszczewski S. Decomposition of macroalgae and the release of nutrient in Admiralty Bay, King George Island, Antarctica. *Polar Biosci* 2004;**17**:26–35.

Nikrad MP, Cottrell MT, Kirchman DL. Growth activity of gammaproteobacterial subgroups in waters off the west Antarctic Peninsula in summer and fall. *Environ Microbiol* 2013;**16**:1513–23.

Olsen L, Ardelan M, Hewes C *et al.* Microbial biogeography during austral summer 2007 in the surface waters around the South Shetland Islands, Antarctica. *Aquatic Microbial Ecol* 2013;**70**:131–40.

Piquet AM-T, Bolhuis H, Davidson AT *et al*. Diversity and dynamics of Antarctic marine microbial eukaryotes under manipulated environmental UV radiation. *FEMS Microbiol Ecol* 2008;**66**:352–66.

Piquet AM-T, Bolhuis H, Meredith MP *et al*. Shifts in coastal Antarctic marine microbial communities during and after melt water-related surface stratification. *FEMS Microbiol Ecol* 2011;**76**:413–27.

Piquet AM-T, Van de Poll WH, Visser RJW *et al*. Springtime phytoplankton dynamics in Arctic Krossfjorden and Kongsfjorden (Spitsbergen) as a function of glacier proximity. *Biogeosciences* 2014;**11**:2263–79.

Quast C, Pruesse E, Yilmaz P *et al*. The SILVA ribosomal RNA gene database project: improved data processing and web-based tools. *Nucleic Acids Res* 2013;**41**:D590–6.

R Core Team. R: *A language and environment for statistical computing. Vienna, Austria: R Foundation for Statistical Computing,* 2014.

Ramette A, Tiedje JM. Multiscale responses of microbial life to spatial distance and environmental heterogeneity in a patchy ecosystem. *P Natl Acad Sci USA* 2007;**104**:2761–6.

Ruiz-González C, Simó R, Sommaruga R *et al*. Away from darkness: a review on the effects of solar radiation on heterotrophic bacterioplankton activity. *Front Microbiol* 2013;**4**: 1–24.

Sailley SF, Ducklow HW, Moeller HV *et al*. Carbon fluxes and pelagic ecosystem dynamics near two western Antarctic Peninsula Adélie penguin colonies: an inverse model approach. *Mar Ecol Prog Ser* 2013;**492**:253–72.

Santos IR, Silva-Filho EV, Schaefer CEGR *et al*. Heavy metal contamination in coastal sediments and soils near the Brazilian Antarctic Station, King George Island. *Mar Pollut Bull* 2005;**50**:185–94.

Singh BK, Bardgett RD, Smith P *et al*. Microorganisms and climate change: terrestrial feedbacks and mitigation options. *Nat Rev Microbiol* 2010;**8**:779–90.

Sutherland WJ, Freckleton RP, Godfray HCJ *et al*. Identification of 100 fundamental ecological questions. *J Ecol* 2013;**101**:58–67.

Smetacek V, Nicol S. Polar ocean ecosystems in a changing world. *Nature* 2005;**437**:362–8.

Turner J, Colwell SR, Marshall GJ *et al*. Antarctic climate change during the last 50 years. *Int J Climatol* 2005;**25**:279–94.

Valdivia N, Díaz MJ, Holtheuer J *et al*. Up, down, and all around: scale-dependent spatial variation in rocky-shore communities of Fildes Peninsula, King George Island, Antarctica. *PLoS One* 2014;**9**:1–12.

Verleyen E, Sabbe K, Hodgson DA *et al*. Structuring effects of climate-related environmental factors on Antarctic microbial mat communities. *Aquat Microb Ecol* 2010;**59**:11–24.

Weisburg WG, Barns SM, Pelletier DA *et al*. 16S ribosomal DNA amplification for phylogenetic study. *J Bacteriol* 1991;**173**:697–703.

Webster NS, Negri AP. Site-specific variation in Antarctic marine biofilms established on artificial surfaces. *Environ Microbiol* 2006;**8**:1177–90.

Weber LH, El-Sayed SZ. Contributions of the net, nano-and picoplankton to the phytoplankton standing crop and primary productivity in the Southern Ocean. *J Plankton Res* 1987;**9**: 973–94.

West NJ, Scanlan DJ. Niche-partitioning of *Prochlorococcus* populations in a stratified water column in the eastern North Atlantic Ocean. *Appl Environ Microb* 1999;**65**:2585–91.

Wilkins D, Yau S, Williams TJ *et al*. Key microbial drivers in Antarctic aquatic environments. *FEMS Microbiol Rev* 2013;**37**:303–35.

Winter C, Matthews B, Suttle CA. Effects of environmental variation and spatial distance on Bacteria, Archaea and viruses in sub-polar and arctic waters. *ISME J* 2013;**7**:1507–18.

Yoon HI, Park BK, Domack EW *et al*. Distribution and dispersal pattern of suspended particulate matter in Maxwell Bay and its tributary, Marian Cove, in the South Shetland Islands, West Antarctica. *Mar Geol* 1998;**152**:261–75.

Zdanowski MK, Zmuda MJ, Zwolska I. Bacterial role in the decomposition of marine-derived material (penguin guano) in the terrestrial maritime Antarctic. *Soil Biol Biochem* 2005;**37**:581–95.

Zeng YX, Zhang F, He JF *et al*. Bacterioplankton community structure in the Arctic waters as revealed by pyrosequencing of 16S rRNA genes. *Anton Leeuw Int J G* 2013;**103**:1309–19.